25. Iterative Least-Squares Lineshape Fitting of ^{1}H-decoupled ^{13}C-DNMR. Spectra

by **Josef Heinzer** and **Jean F.M. Oth**

Laboratory for Organic Chemistry, Swiss Federal Institute of Technology, Universitätstrasse 16 CH-8092 Zürich

(16.VII.79)/(24.X.80)

Summary

Iterative least-squares lineshape fitting of ^{1}H-decoupled ^{13}C-DNMR. spectra is advantageously used for the investigation of symmetrical or asymmetrical intramolecular (two-structure) exchange processes. The least-squares procedure adopted allows the following parameters to be either optimized by computer or kept constant (according to experimental conditions): the nuclei populations (taking into account line intensity effects resulting from differences in spin-lattice relaxation times and/or *Overhauser* enhancements), the corresponding chemical shifts and natural linewidths (characterizing the sites undergoing exchange), the fractional population of one structure (in the case of asymmetrical exchange), one of the chemical rates, the base-line position, and the base-line tilt. The relative sensitivity of the lineshape with respect to the fitted parameters as well as the importance of correlations among these parameters have been investigated and tested with examples. The reliability of the kinetic parameters as obtained by the iterative least-squares lineshape fitting procedure is discussed.

Introduction. - Proton decoupled ^{13}C-DNMR. spectroscopy proves to be a very suitable tool for the investigation of intramolecular exchange processes in solution [1-10]. The absence of spin-spin couplings allows complete analyses of even complex exchange-broadened spectra. In addition, the generally larger ^{13}C-chemical shift differences compared to those of ^{1}H-NMR. increase the temperature interval where dynamic behaviour can be observed. These advantages of ^{13}C-DNMR. spectroscopy are counterbalanced to some extend by inconveniences resulting from variable spin-lattice relaxation times and from *Overhauser* effects. Both effects modify the lineshape in such a manner that the areas of the lines are no longer proportional to the nuclei populations. The generally low signal-to-noise ratio of ^{13}C-exchange-broadened spectra lessens the reliability of the fitted parameters.

Iterative least-squares lineshape fitting of experimental spectra by adjusting the exchange rate has been described by several authors [11-15]. Peak separations [13] have also occasionally been varied by computer in order to take into account their

0018-019X/81/1/0258-21$01.00/0

temperature dependence. In 1973, a program (CLSFIT) was presented which refines by iterative least-squares lineshape fitting spin-site frequencies and populations, pseudo-first-order rates and apparent linewidth of uncoupled or weakly coupled (first-order approximation) spin systems [16]. Meanwhile, iterative lineshape fitting made almost fully automatic, has become a powerful tool in analyzing ^{1}H-NMR. spectra [17–19].

In this paper, we present a general procedure and the lay-out of a program called CNMREX for analyzing ^{13}C-DNMR. spectra subjected to variable spin-lattice relaxation times and/or *Overhauser* effects. The iterative part of CNMREX applied a modified *Marquardt* algorithm [20] treating the integral of the spectrum as a variable parameter [21]. *Marquardt's* concept of choosing the parameter correction vector such that its direction lays somewhere between the first-order *Taylor*-series direction and the direction of steepest descent was altered by *Jones* [22] in such a way that this correction vector is build up algebraically from the components of the two directions. As has been shown by *Stephenson & Binsch* [17] [18] *Jones'* method, called spiral algorithm, proves to be very successful in NMR. lineshape analysis. Numerous tests revealed that this spiral algorithm is well suited to the analysis of ^{13}C-DNMR. spectra. The new version of CNMREX, therefore, follows about the same line as has been outlined by above authors, however, retaining in some cases a small damping in order to reduce parameter correlations.

Two test calculations and two practical appliations are also presented in detail.

Theory. – *The lineshape function.* The lineshape of a proton decoupled ^{13}C-DNMR. spectrum can be described by the function:

$$I(\nu, \mathbf{p}) = I_S + a(\nu)\ I_T + c I_C(\nu) \tag{1}$$

where $\mathbf{p}$ is a vector in the n_P-dimensional parameter space. I_S is the base-line shift at the low field end ν_n of the spectrum whereas I_T is the base-line tilt which is determined from the base-line shift at the high field end ν_1 of the spectrum by subtracting I_S. $a(\nu)$ is assumed to express a linear relationship $a(\nu) = (\nu - \nu_n)/(\nu_1 - \nu_n)$. The scaling factor c is obtained from the areas of the integrated experimental (subtracting the trapezoidal area due to the base-line shift and tilt) and the integral of the theoretical spectrum. The theoretical lineshape $I_C(\nu)$ is calculated according to:

$$I_C(\nu) = -\mathrm{Re}\left[\sum_{j=1}^{n_G} \mathbf{G}_j^T\, \mathbf{M}_j^{-1} \mathbf{P}\right]. \tag{2}$$

The sum indicates that there are n_G groups of nuclei (sites) exchanging among each other (see the applications). $\mathbf{G}_j^T$ is a row vector representing the nuclei populations within each group j (it should be noted that in the ^{1}H decoupled ^{13}C-DNMR. spectroscopy these populations may have to be varied in order to compensate effects of variable spin-lattice relaxation times and/or *Overhauser* enhancements which affect the signal intensities). $\mathbf{P}$ is a column vector built up from the fractional populations of the exchanging structures. The non-*Hermitian* matrix $\mathbf{M}_j$ [16] [23–25], formulated in *Liouville* space, reads:

$$\mathbf{M}_j = 2\pi\, i\, (\boldsymbol{\nu}_j - \nu \mathbf{E}) - \pi \Delta \boldsymbol{\nu}_j + \mathbf{X}. \tag{3}$$

The elements of the diagonal matrix ν_j and $\Delta\nu_j$ consist of the transition frequencies and natural linewidths, respectively, observed for the nuclei (sites) of group j. **X** is the non-diagonal intramolecular exchange matrix given by $X_{kl} = -\delta_{kl}\sum_{n\neq k}^{n_s} k_{kn} + (1-\delta_{kl})k_{lk}$ where $k_{lk}(k_{kn})$ denotes the time probability density (or rate) for a ^{13}C-nuclei to exchange from site j,l into j,k (j,k into j,n); δ_{kl} represents the *Kronecker* symbol.

By decomposing $\mathbf{M}_j$ into a constant matrix $\mathbf{B}_j$ and a scalar matrix $2\pi i\nu\mathbf{E}$ [24] [26-28] and assuming that $\mathbf{B}_j$ can always be reduced to a diagonal matrix we can write the lineshape function as:

$$\begin{aligned} I_C(\nu) &= -\mathrm{Re}\left[\sum_{j=1}^{n_G}\sum_{k=1}^{n_S} \mathbf{G}_j^T\,\mathbf{U}_{j,k}\,(\Lambda_{j,k}-2\pi i\nu)^{-1}\,\mathbf{U}_{j,k}^{-1}\,\mathbf{P}\right] \\ &= -\mathrm{Re}\left[\sum_{j=1}^{n_G}\sum_{k=1}^{n_S} \mathbf{S}_{j,k}\,(\Lambda_{j,k}-2\pi i\nu)^{-1}\right] \\ &= -\mathrm{Re}\left[\sum_{j=1}^{n_G} \mathbf{S}_j\mathbf{Q}_j(\nu)\right] \end{aligned} \tag{4}$$

where $\Lambda_{j,k}$ and $\mathbf{U}_{j,k}$ are the eigenvalues and the eigenvectors of $\mathbf{B}_j$, respectively. $\mathbf{S}_j$ (independent of ν) and $\mathbf{Q}_j(\nu)$ are complex vectors.

Least-squares lineshape fitting. – The least-squares procedure used originally was based on *Marquardt's* method:

$$\begin{aligned} \mathbf{p}_{k+1} &= \mathbf{p}_k + (\mathbf{H}_k^T\mathbf{H}_k + \lambda\,\mathbf{V})^{-1}\,\mathbf{H}_k^T[\mathbf{I}-\mathbf{I}(\mathbf{p}_k)] \\ &= \mathbf{p}_k + (\mathbf{A}_k + \lambda\,\mathbf{V})^{-1}\,\mathbf{q}_k \end{aligned} \tag{5}$$

where $\mathbf{p}_{k+1}$ denotes the iterated parameter vector calculated recursively from the current $\mathbf{p}_k$. $\mathbf{H}_k$ is the $n\times n_P$ matrix whose elements are $g_{ir}(\mathbf{p}_k) = \partial I_i(\mathbf{p}_k)/\partial p_r$. When $\lambda = 0$ *Marquardt's* method reduces for any matrix $\overline{\mathbf{V}}$ to ordinary first-order *Taylor*-series least-squares (searching along the direction $\delta\mathbf{p}_k = \mathbf{A}_k^{-1}\,\mathbf{q}_k$). A large λ corresponds to a short step which for $\lambda\to\infty$ and provided that $\mathbf{V}=\mathbf{E}$ coincides with the direction of steepest descent $\mathbf{q}_k$. Replacing **V** by a matrix containing merely the diagonal elements of $\mathbf{A}_k$ we get the modified algorithm described in an earlier publication [21] which corresponds more or less to a search along $\delta\mathbf{p}_k$.

In *Jones'* method [22] the search points are constructed simply by vector addition:

$$\mathbf{p}_{k+1} = \mathbf{p}_k + s\,t_l\,[-\mu_m(|\delta\mathbf{p}_k|/|\mathbf{q}_k|)\mathbf{q}_k + (1-\mu_m)\delta\mathbf{p}_k]; \tag{6}$$

with

$$\begin{gathered} s = [1-\theta\cot\beta-(1-\gamma\cot\beta)(\theta/\gamma)^2]\cos\theta/(1-\mu_m+\mu_m\cos\gamma); \\ \tan\theta = \mu_m\sin\gamma/(1-\mu_m+\mu_m\cos\gamma); \\ \cos\gamma = \mathbf{q}_k\,\delta\mathbf{p}_k/(|\mathbf{q}_k|\,|\delta\mathbf{p}_k|); \\ \beta = \gamma/2; \\ \mu_1 = 0.1, \\ \mu_{m+1} = 2\mu_m/(1+\mu_m)\ (m=1,2,3,4). \end{gathered}$$

Each iteration cycle k starts with a search at $\delta\mathbf{p}_k$ ($t_0=1$, $\mu_0=0$). If this search is not successful up to four points (specified by $\mu_1,\ldots,\mu_4$) along the spiral $t_0=1$, and five points ($\mu_0,\ldots,\mu_4$) along the spirals $t_1=1/3$, and eventually $t_2=1/9$, are con-

sulted. Finally, points on $\mathbf{q}_k$ itself are searched. The search is terminated and the iteration cycle restarted as soon the program has found a better solution $\chi^2(\mathbf{p}_{k+1}) < \chi^2(\mathbf{p}_k)$. The program CNMREX does not perform interpolations between neighbouring search points. The advantage of this so called spiral algorithm mainly consists in the fact that a given area is searched systematically (and automatically) point by point making it possible to jump over 'hills' and 'valleys' in the error function.

The definitions of statistical data such as standard deviation used as convergence criteria, R factor, confidence limits, and correlation matrix (see also text books) have already been outlined in earlier publications [21] [29].

Parameter sensitivities. – In the course of quantitative analyses of exchange-broadened spectra it proved very helpful to be provided with relative parameter sensitivities (numbers relating the amount of lineshape change to the variation of specific parameters). Among different methods which could be chosen to express such sensitivities the following one is proposed:

$$\Delta\mathbf{s} = [\mathbf{A}_d]^{1/2}\,\Delta\mathbf{p} \tag{7}$$

(For other sensitivity measures compare [30] or [31]). Δs_r is called the sensitivity of the parameter $\mathbf{p}_r$. $\mathbf{A}_d$ contains the diagonal elements of $\mathbf{A}$. In order to relate the sensitivities among each other all $\Delta\mathbf{p}_r$ are set equal to $\mathbf{p}_r/100$.

Applications of the parameters sensitivities will be discussed in the examples below.

Program CNMREX. – The least-squares procedure is limited to 23 simultaneously variable parameters (the actual number of parameters may be as large as 40) and to 1000 digital points. On a CDC 6400/6500 the computing time for adjusting one parameter amounts to about 1 second per iteration and 1000 data points. The output consists of a list of the optimized parameters together with standard error, R factor, parameter errors, correlation matrix, and parameter sensitivities (printed out as $\log_{10}\Delta S_r$). Print plot and /or plot output is obtained according to options read in.

The program does not read data from tape; it rather uses the modified subroutine READDA for incorporating data prepared by a small computer. We find that it will be best (at least for our purposes) to preprocess data on a small computer in order to keep the size and the core memory of CNMREX as small as possible.

Table 1. *Parameters of example A (B)*

Parameters j	1	2	3	4
G_j	1	1	1	1
$\nu_{j,1}$ [Hz]	280	210	215	180
$\Delta\nu_{j,1}$ [Hz]	1	2	1	1
$\nu_{j,2}$ [Hz]	20	30	165 (175)	170
$\Delta\nu_{j,2}$ [Hz]	1	2	1	1
P_1	0.7 (0.9)			
k_{12} [s^{-1}]	0.01 to 1,000,000			
I_S [mm]	0.0 (10.0)			
I_T [mm]	0.0 (10.0)			

The algorithm adopted in the program has been selected in view of future extensions of the program to more complicated exchange problems.

Test examples. In order to gain some insight into the reliability of the parameter values as obtained from lineshape fitting, fictitious spectra with a signal-to-noise ratio of 25/1 were tested.

Example A. The first example deals with the asymmetric exchange (two non-isometric structures) of four sites of one structure with four sites of the other (number of pairs of exchanging sites: $n_G = 4$). The exchange rates k_{12} and k_{21} are related to the fractional populations P_1 and P_2 of structures 1 and 2 by: $k_{21} = k_{12} P_1/P_2$, $P_1 + P_2 = 1$. The total number n_P of adjustable parameters $\{G_{j,k}, \nu_{j,k}, \Delta\nu_{j,k}; P_1, k_{12}; I_S, I_T\}$ amounts to 24 if the weights $G_{j,1}$ and $G_{j,2}$ are set equal to $G_j = G_{j,1} = G_{j,2}$ ($j = 1, \ldots, 4$). These 24 parameters are listed in *Table 1*.

Starting the lineshape analysis at slow exchange (if at all possible) one gets supplied with the refined parameters, their sensitivities and correlations. These data allow one to decide which of the parameters should be optimized in the next run. Normally, the number of simultaneously adjustable parameters gradually decreases as the coalescence region is approached. The smallest number of variable parameters coincides with the coalescence region. In the fast exchange domain some of the parameters may become strongly correlated ($|C_{rs}| > 0.75$) with each other. This will be the case for the chemical shifts $\nu_{j,k}$ in:

$$\bar{\nu}_j = P_1 \nu_{j,1} + (1 - P_1) \nu_{j,2}$$

and for the natural linewidths $\Delta\nu_{j,k}$ in:

$$\Delta\bar{\nu}_j = P_1 \Delta\nu_{j,1} + (1 - P_1) \Delta\nu_{j,2}.$$

The averaged chemical shifts $\bar{\nu}_j$ and linewidths $\Delta\bar{\nu}_j$, respectively, observed at fast asymmetric exchange are functions of three parameters. Variation of any one of these three parameters would adjust either $\bar{\nu}_j$, or $\Delta\bar{\nu}_j$ to the experimental value. P_1 is only meaningfully variable (at fast exchange) in such cases where $\nu_{j,1}$ and $\nu_{j,2}$ are hold constant which implies that both chemical shifts have to be extrapolated from values obtained at slow exchange. $\Delta\bar{\nu}_j$ may be adapted by varying one of the $\Delta\nu_{j,k}$ (if its sensitivity is high enough).

In order to illustrate how the lineshape is sensitive with respect to variation of the different parameters, we plotted the $\log_{10} \Delta S_r$ values for $r = G_2$, $\nu_{1,k}$, $\nu_{4,k}$, $\Delta\nu_{1,k}$, $\Delta\nu_{4,k}$, P_1, and k_{12} *versus* exchange rates ($\log_{10} k_{12}$) covering the whole range of lineshape modification ($\Delta p_r = p_r/100$). Sensitivities left out in *Figure 1* indicate either strongly correlating or badly reproducible parameters. The strong correlation was removed by keeping the parameter(s) of the less populated structure 2 constant. These sensitivity plots indicate that, in full agreement with practical experience: i) the lineshape is extremely sensitive to a variation of the resonance frequency characteristics of the sites; the sensitivity is greatest at the slow and the fast exchange domain and smallest at coalescence; ii) the lineshape is highly sensitive to a variation of the (larger) fractional population P_1 of one of the two structures in dynamic equilibrium (any correction of P_1 will affect P_2 through renormalisation as well); iii) the lineshape is (very) sensitive to a variation of the exchange rate k_{12} (and k_{21}) only within a certain range (in example A: $1 < k_{12} < 10^5\ s^{-1}$); iv) the

sensitivity of the linewidths is appreciably large only in the region of very slow or very fast exchange ($\Delta\nu_{1,1}$ in example A: $2 > k_{12} > 10^4\ s^{-1}$).

Since the correct values of k_{12} are known for each of the tested spectra, it is possible to check the performance of the optimization procedure by comparing the true value k_{12} with that obtained from a fitting process performed on the listed

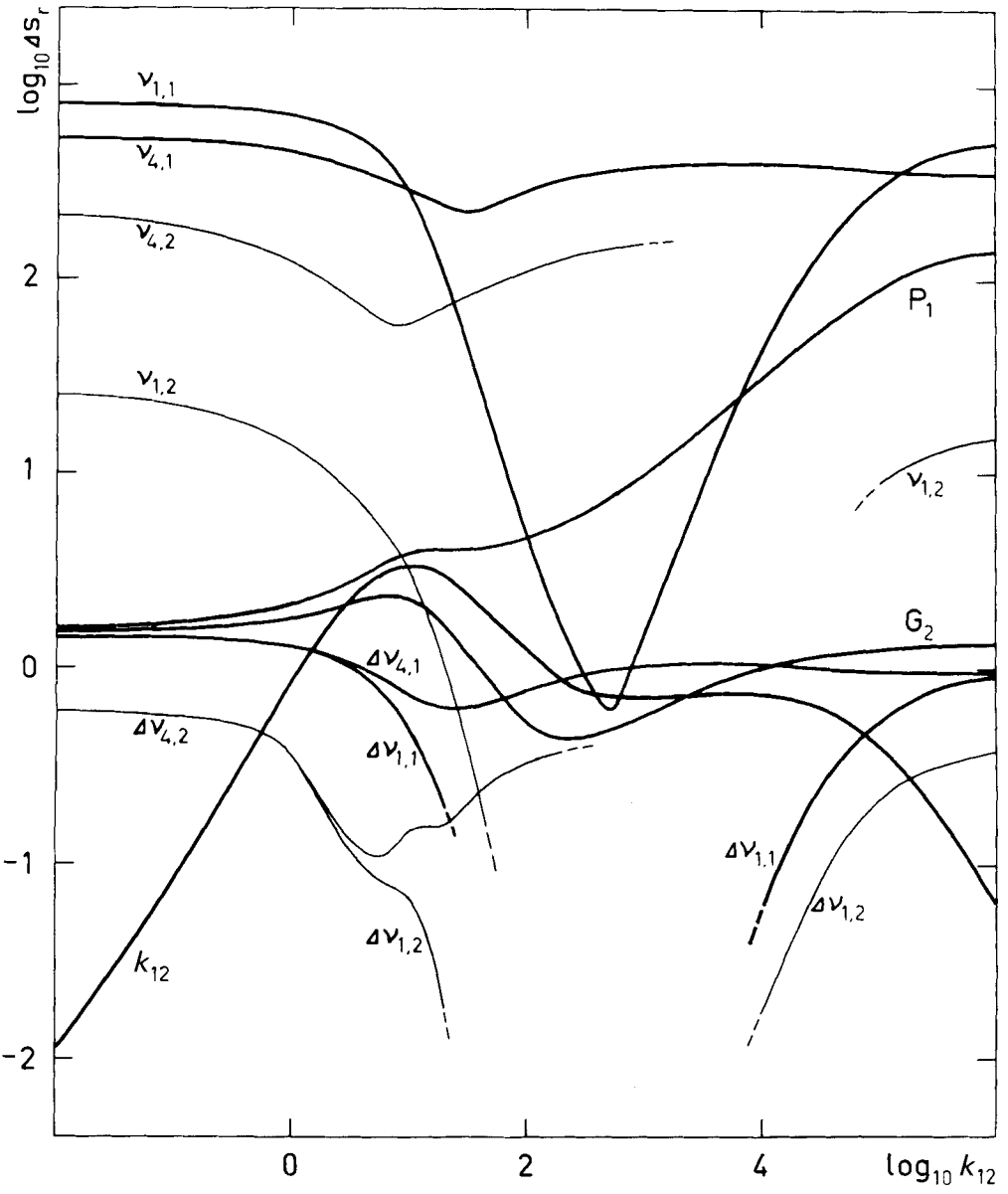

Fig. 1. *Parameter sensitivities of example A*. Thin curves indicate parameters of structure 2

parameters (except I_S and I_T). After a few iterations allowing the errors to propagate into the parameters, a new 'best' set was obtained. The relative error Δk_{12} connected with this calculated 'best' value k_{12}^{calc} is defined by:

$$\Delta k_{12} = |k_{12} - k_{12}^{calc}| / k_{12}.$$

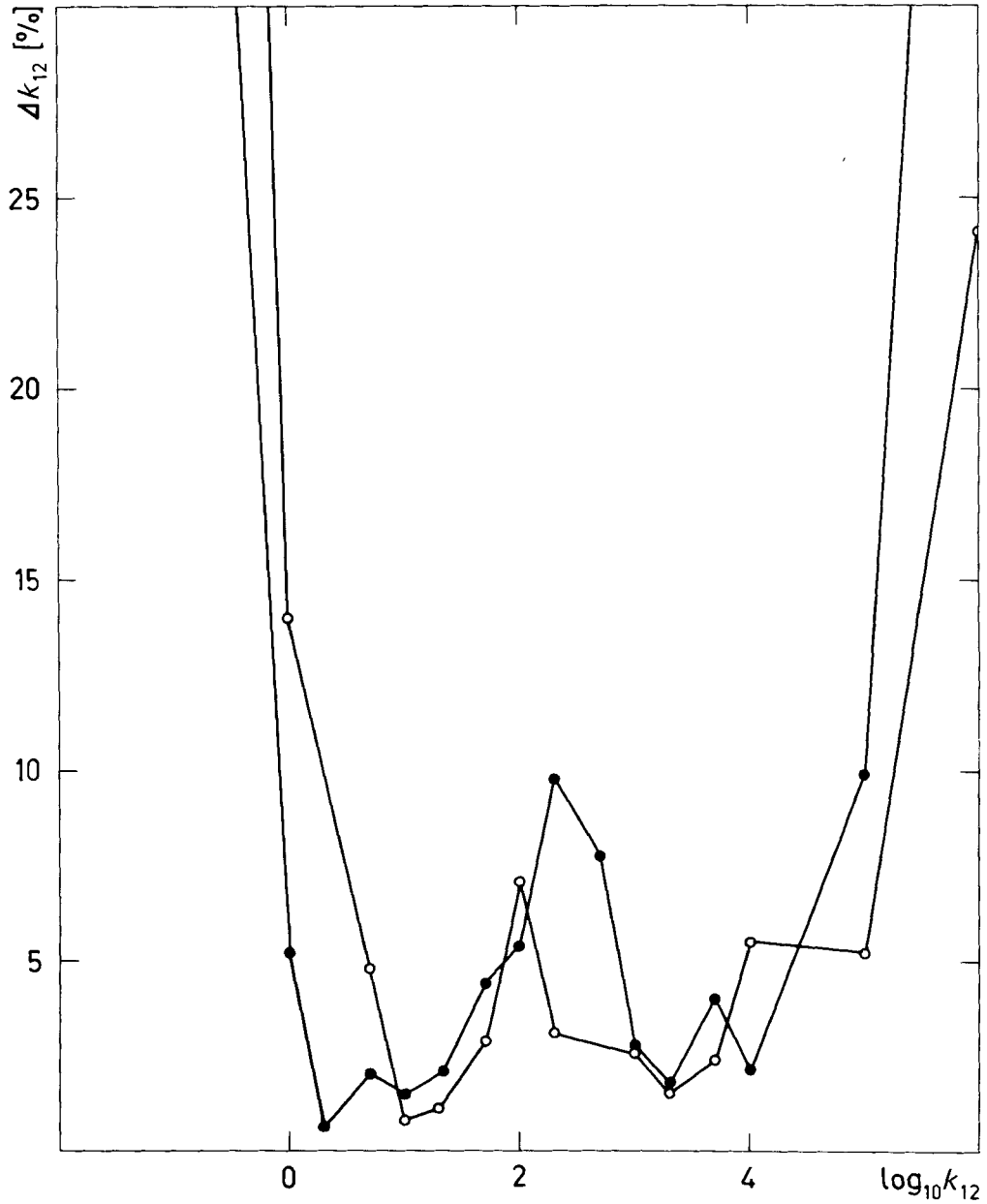

Fig. 2. *Relative errors* Δk_{12} [%] *of example A* (○) *and example B* (●)

Figure 2 (example A is indicated by circles) shows indeed that the smaller errors are obtained in the region of maximum sensitivity $\Delta s_{k_{12}}$ *(Fig. 1)*.

In order to calculate the *Arrhenius* parameters (E_A and A) it would be, therefore, meaningful to consider (only) rates located in the region of maximum sensitivity. Alternatively, the evaluated rates might be weighted in an *Arrhenius* regression as follows:

$$w_T = (\Delta s_{k_{12}})_T / (\Delta s_{k_{12}})_{max}$$

where w_T is the weight of k_{12} determined by fitting the spectrum recorded at temperature T, $(\Delta s_{k_{12}})_T$ stands for the sensitivity of the rate k_{12} at temperature T and $(\Delta s_{k_{12}})_T$ for the maximum value of the sensitivities $\Delta s_{k_{12}}$. The weights w_T defined above will, however, not take into account errors arising from inaccurately determined temperature dependent chemical shifts, populations, natural linewidths, and site populations.

Example B. In the second example, the same parameters as in the first example were selected except for the chemical shift $\nu_{3,2}$, the population P_1 (implying $P_2 = 1 - P_1$), the base-line shift I_S, and the base-line tilt I_T which were replaced by the ones given in brackets in *Table 1*. The ratio of the populations $P_1/P_2 = 9$ indicating a rather asymmetric exchange, was chosen such that in the slow exchange limit ($k_{12} < 5\ s^{-1}$) the smallest ^{13}C-signal ($\nu_{2,2}$) could be considered as detectable. Its signal-to-noise ratio is:

$$S/N = 25/[(P_1/P_2)(\Delta\nu_{2,2}/\Delta\nu_{1,2})] = 1.39$$

(the signal-to-noise ratio of a signal of the most populated structure 1 is 25/1). The slow rate is referred to by k_{12}. In *Figure 3*, the lineshape sensitivities with respect to variation of the parameters $r = G_1$, G_4, $\nu_{1,k}$, $\nu_{4,k}$, $\Delta\nu_{1,k}$, $\Delta\nu_{4,k}$, P_1, and k_{12} ($\Delta p_r = p_r/100$ as in example A) are plotted as functions of $\log_{10} k_{12}$. The sensitivities of the base-line shift and tilt remained constant ($\log_{10} \Delta s_{I_S} = 0.52$ and $\log_{10} \Delta s_{I_T} = 0.30$). As a consequence of the strongly asymmetric exchange the sensitivities referring to the parameters $\nu_{j,1}$ and $\Delta\nu_{j,1}$ of structure 1 are much larger than those of structure 2 (thin curves). The sensitivity of the exchange rate k_{12} is again greatest just below coalescence.

The relative errors Δk_{12}, plotted in *Figure 2* (black circles) *versus* $\log_{10} k_{12}$, were determined from least-squares fits using the true parameters as initial parameters. The Δk_{12} values were again calculated by means of the formula outlined above using the iterated 'best' k_{12}^{calc} values. *Figure 2* indicates that the rates estimated below and above but close to coalescence have the smallest errors. In this exchange, the relative errors seem to be greater than in the first example.

Fitting of experimental spectra. – The following two experimental examples have been chosen in view of explaining computational details rather than chemical aspects which will be published elsewhere. All spectra analysed were digitalized by hand.

Example C. The dianion of tribenzo[12]annulene ($I^=$) undergoes a conformational exchange in which two isometric structures are involved *(Fig. 4)*. This conformational mobility [32] is due to a synchronous rotation of the three –CH=CH– fragments of the [12] annulene around the bonds connecting these

fragments to the benzene rings. *Figure 4* reproduces the exchange diagram characterizing this dynamic behaviour (the letters individualize the different

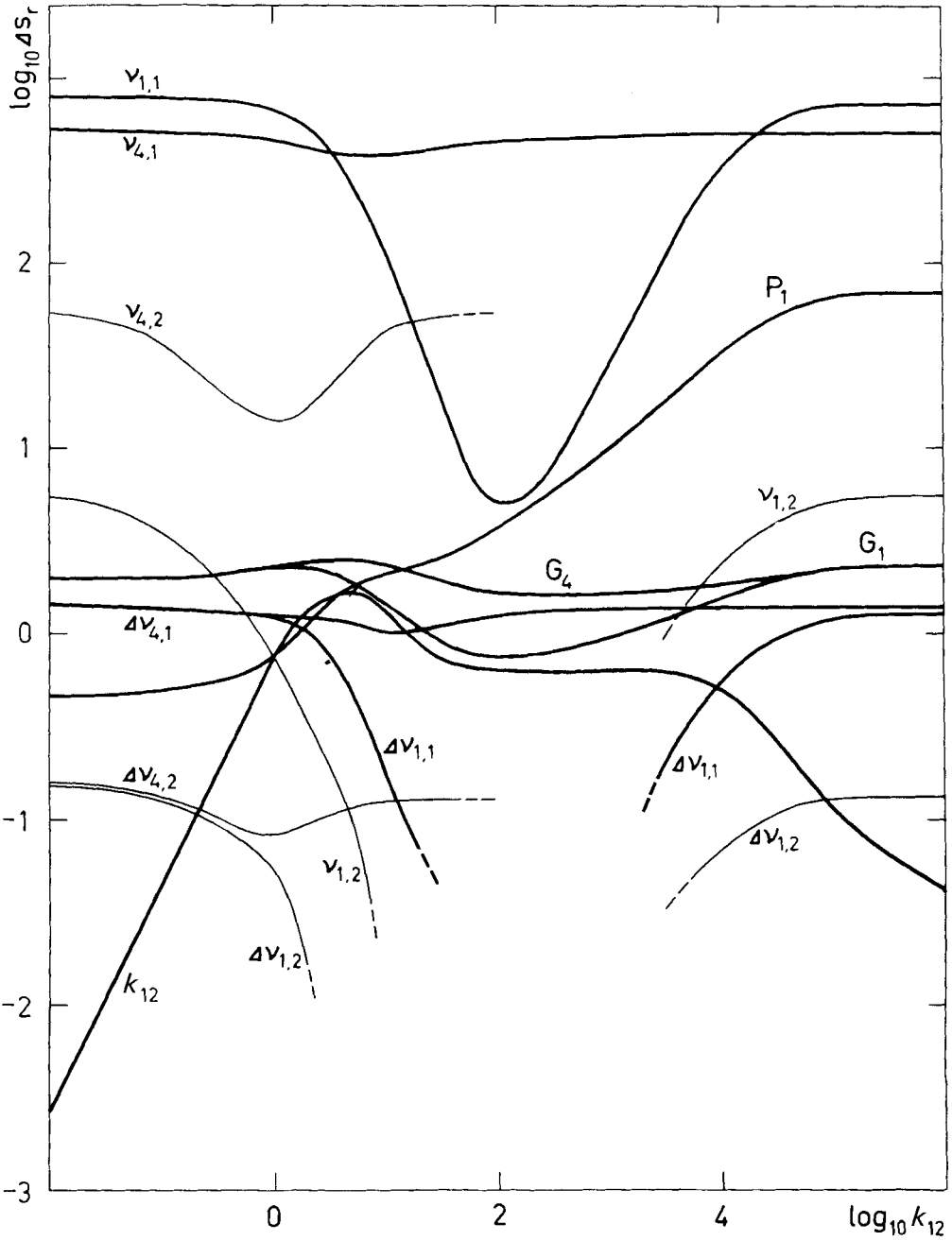

Fig. 3. *Parameter sensitivities of example B*

^{13}C-nuclei; the numbers identify the magnetic environments or sites). Due to a threefold symmetry axis the total number of sites reduces to 8, each one being occupied by 3 nuclei. We thus have here a symmetric exchange of 4 pairs of sites ($n_G = 4$). At low temperature (-60°C) the ^{13}C-DNMR. spectrum consists of 8 lines *(Fig. 5)*. A 4 line spectrum is obtained by raising the temperature above 20°C.

The ^{13}C-spectra of $I^=$ (solved in THF-d_8) have been recorded by means of a *Varian* XL-100 spectrometer (lock signal: ^{2}H/THF-d_8. high field side; reference signal: TMS).

The spectra in the range of -60 to 31°C were fitted by noting that: $P_1 = P_2 = 0.5$ and assuming that the sites of all CH groups (1, 2; 5, 8; 6, 7) are equally populated:

$$G_{j,1} = G_{j,2} = 1 \text{ for all j (except 2).}$$

$G_2 = G_{2,1} = G_{2,2}$ was allowed to vary since the signal intensity of the quarternary C-atoms (sites 3 and 4) depends upon temperature.

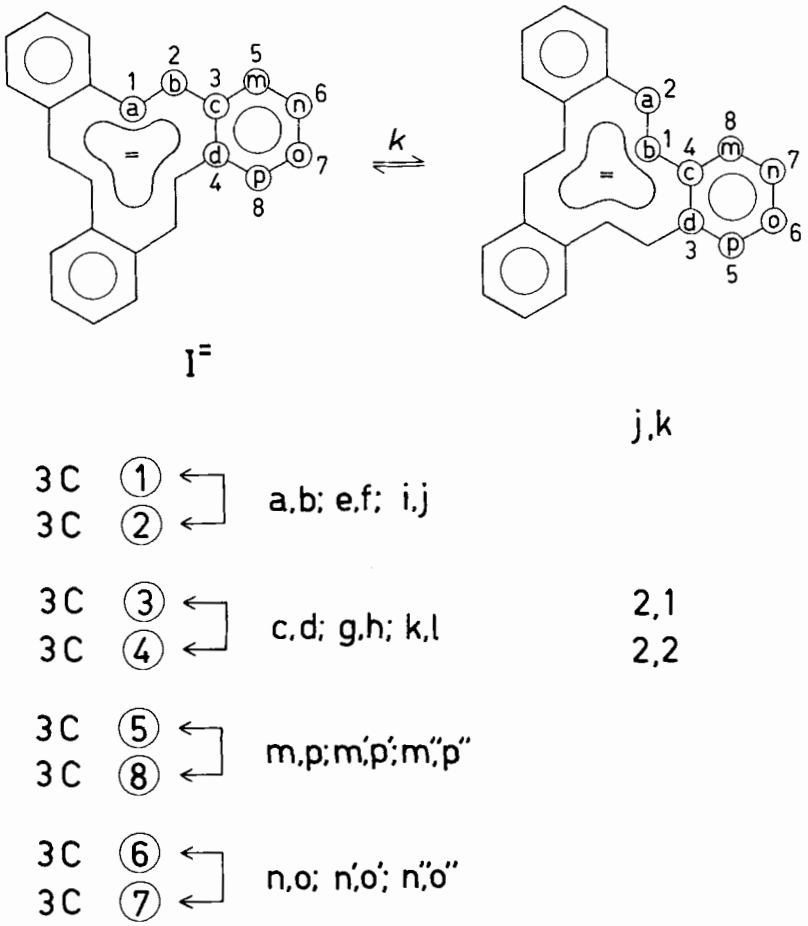

Fig. 4. *Exchange diagram of example C*

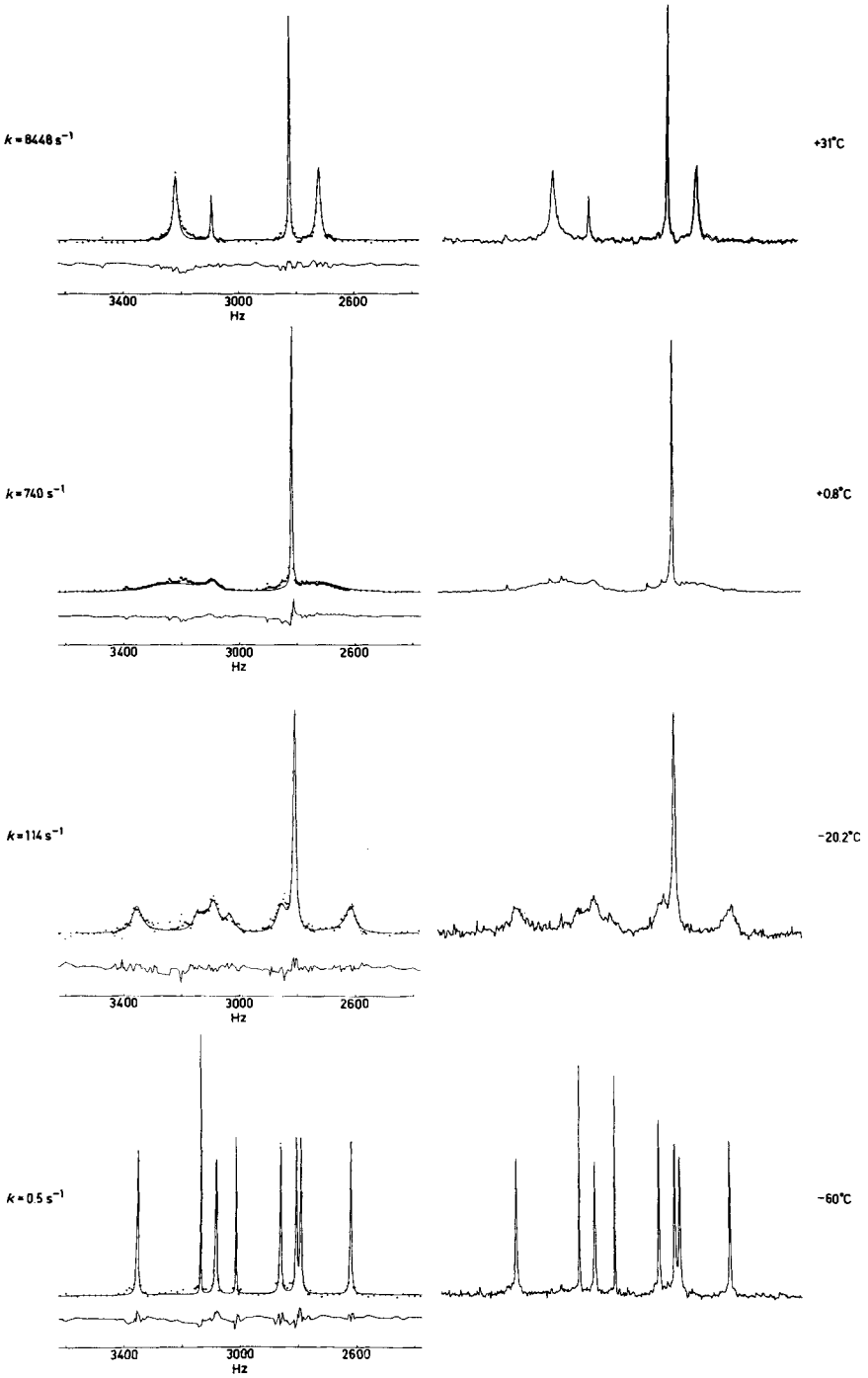

Fig. 5. Experimental and simulated spectra at various temperatures (Example C)

In order to calculate the rates correctly, the temperature dependence of the chemical shifts and if possible of the linewidths have to be taken into account.

The chemical shifts were assumed to vary linearly with temperature:

$$\nu_{j,k}(t) = \nu^0_{j,k} + b_{j,k}\, t.$$

$\nu^0_{j,k}$ and $b_{j,k}$ were determined from the least-squares adjusted chemical shifts of the four lowest temperatures (−60, −39.9, −30.1, −20.2°C). The values of $\nu^0_{j,k}$ and $b_{j,k}$ are listed in *Table 2*. Deviations of the extrapolated chemical shifts at fast exchange due to calibration errors were adjusted by allowing the computer to shift both frequences by half of the least-squares correction $\delta\nu_{j,1}/2$ ($\nu_{j,2}$ not varied).

Determination of the linewidths turned out to be somewhat questionable. The region where $\Delta\nu_1$ or $\Delta\nu_2$ ($\Delta\nu_1 = \Delta\nu_{1,k} = \Delta\nu_{3,k} = \Delta\nu_{4,k}$; $\Delta\nu_2 = \Delta\nu_{2,k}$) could be adjusted by least-squares was strictly limited to low or high temperature.

It is interesting to note that the different parameter sensitivities for $r = G_2$, $\nu_{j,1}$, $\Delta\nu_1$, $\Delta\nu_2$, and k as functions of $\log_{10}k$ (*Fig. 6*, with $\Delta p_r = p_r/100$) show an analogous behaviour as those observed in our first two fictitious examples. From *Figure 6* one might deduce, for instance, that $k = 0.5$ s^{-1} lies just outside the range where a least-squares determination is possible. Indeed, an accurate determination of such a small rate could not be expected considering the small number ($n = 156$) of data points representing the digital spectrum.

In most cases it was necessary to start the iterations with a relatively small number of parameters. Once a sufficient degree of agreement between the

Table 2. *Temperature dependence of the chemical shifts* (Example C)

Chemical shifts j,k	Tribenzo[12]annulene dianion ($I^=$) $\nu^0_{j,k}$ [Hz]	$b_{j,k}$ [Hz/°C]	Correlation
$\nu_{1,1}$	3354.7	−0.0376	−0.9758
$\nu_{1,2}$	3085.7	0.0003	0.0071
$\nu_{2,1}$	3153.5	0.2399	0.9969
$\nu_{2,2}$	3029.3	0.2162	0.9976
$\nu_{3,1}$	2853.5	−0.1566	−0.9797
$\nu_{3,2}$	2609.5	−0.1883	−0.9826
$\nu_{4,1}$	2823.7	0.2585	0.9761
$\nu_{4,2}$	2801.7	0.1518	0.9776

Table 3. *Kinetic data of the conformational mobility of* $I^=$ (Example C).

E_A [kJ/mol]	$\log_{10}A$	$\Delta H^{\neq}$ [kJ/mol]	$\Delta S^{\neq}$ [J/(mol. grad)]	$\Delta G^{\neq}$ (25°C) [kJ/mol]	K(25°C) [s^{-1}]
56.2 ±1.3[a]	13.5 ±0.25[a]	54.1 ±1.3[a]	7.2 ±2.5[a]	51.94 ±0.38[a]	4893.0 ±742.0[b]

a) Calculated by means of $T_1 = 304$ K, $\sigma_{T_1} = \pm 0.2$ K; $T_2 = 213$ K, $\sigma_{T_2} = \pm 0.4$ K; $\sigma_{K_1}/K_1 = \pm 0.1$; $\sigma_{K_2}/K_2 = \pm 0.2$.

b) $\sigma_K/K = \sigma_{\Delta G^{\neq}}/RT$.

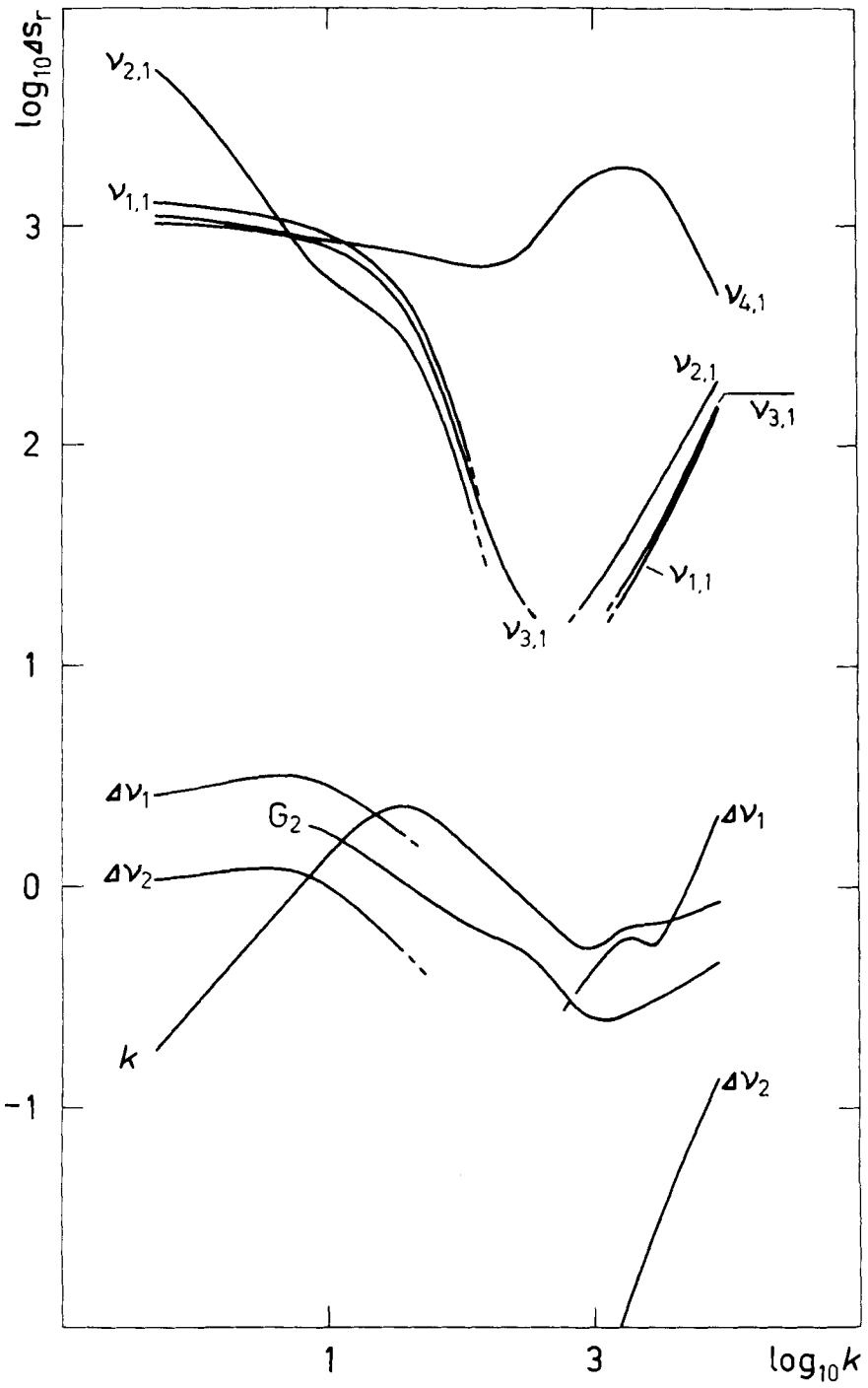

Fig. 6. *Parameter sensitivities of example C*

calculated and observed spectrum is achieved, it might be more convenient and time saving to refine as many parameters as possible.

Figure 7 shows the relative intensity (site population) of the quarternary C-atoms (sites 3 and 4) as a function of temperature (the intensities of the other signals are normalized to unity).

The rate constants were regressed by linear least-squares fitting to the *Arrhenius* and to the *Eyring* equation, using the weights $w_T = (\Delta s_k)_T/(\Delta s_k)_{max}$. The kinetic parameters obtained are listed in *Table 3*. The errors stated in *Table 3* are calculated from the errors of the highest (T_1) and the lowest (T_2) measured temperature and the errors of the corresponding rates $k(T_1) = K_1$, $k(T_2) = K_2$ using the formulas [33] given in the Appendix.

Example D. A final application of the program CNMREX demonstrates the ^{13}C-DNMR. spectrum least-squares analysis of the interconverting tautomeric system of *Figure 8* [34]. Rapid transformation of the isomers II into *trans*-1,2-divinyl-3,5-cyclohexadiene [34] excluded ^{13}C-NMR. measurements above 65°C [35]. (*Varian* XL-100 spectrometer; solvent: CD_2Cl_2; lock signal: $^2H/CD_2Cl_2$, reference signal: TMS). The effect of the asymmetric exchange upon the magnetic sites of II_1 and II_2 (characterized by circles) can be deduced from *Figure 8*.

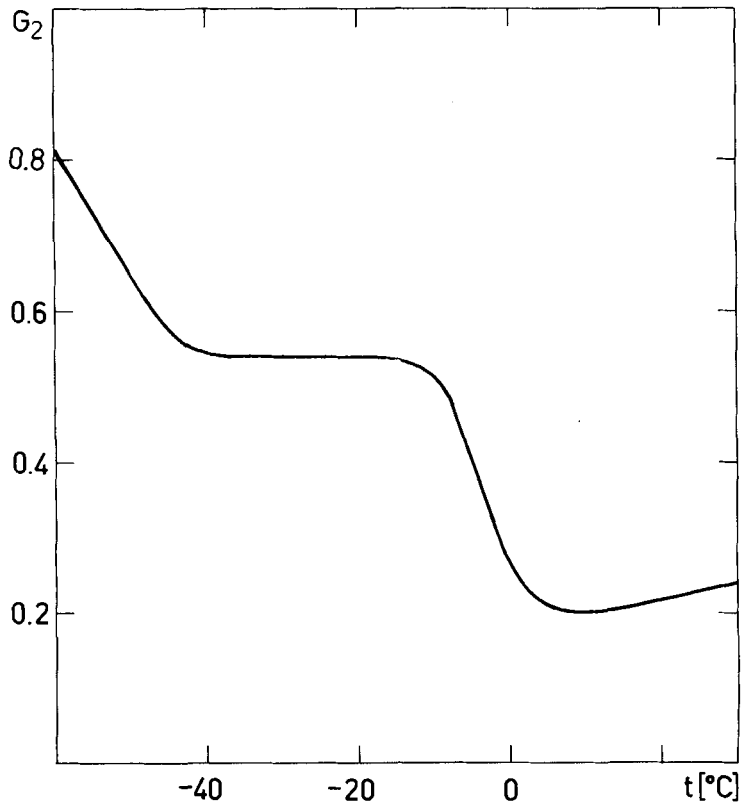

Fig. 7. Temperature dependent site population $G_2 = G_{2,1} = G_{2,2}$ (Example C)

The lineshape of $II_1 \rightleftharpoons II_2$ arising from the vinyl (three sets in II_1, four in II_2) and from the nonvinyl (two sets in II_1, one in II_2) C-atoms were analyzed separately at various temperatures in the range of -20 to 65.7°C assuming that:

$$G_j = G_{j,k} = 1 \text{ (except } G_{1,1})$$

$$\Delta\nu_2 = \Delta\nu_{2,k} = \Delta\nu_{3,k} = \Delta\nu_{4,k}, \text{ and } \Delta\nu_5 = \Delta\nu_{5,k}$$

with k being equal to 1, 2; likewise:

$$\Delta\nu_2 = \Delta\nu_{1,2} \text{ and } \Delta\nu_5 = \Delta\nu_{1,1}.$$

The site population $G_{1,1}$ turned out to be temperature dependent ($G_{1,1} < 1$).

If necessary, the chemical shifts were calculated as in example C by using a linear relation. The values of $\nu^0_{j,k}$ and $b_{j,k}$, listed in *Table 4*, were determined by least-squares from calibrated chemical shifts at -70, -20, 9.77, 20.1, and 25.1°C.

The linewidths $\Delta\nu_2$ and $\Delta\nu_5$ were evaluated either by least-squares where possible or determined from the lines of the decomposition product (with linewidth $\Delta\nu_d$) supposing that $\Delta\nu_j = \Delta\nu_d$.

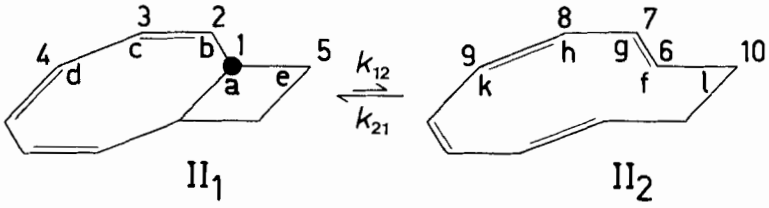

			j,k
2C	①	a,a′	1,1
2C	⑥	f,f′	1,2
2C	②	b,b′	
2C	⑦	g,g′	
2C	③	c,c′	
2C	⑧	h,h′	
2C	④	d,d′	
2C	⑨	k,k′	
2C	⑤	e,e′	5,1
2C	⑩	l,l′	5,2

Fig. 8. *Exchange diagram of example D*

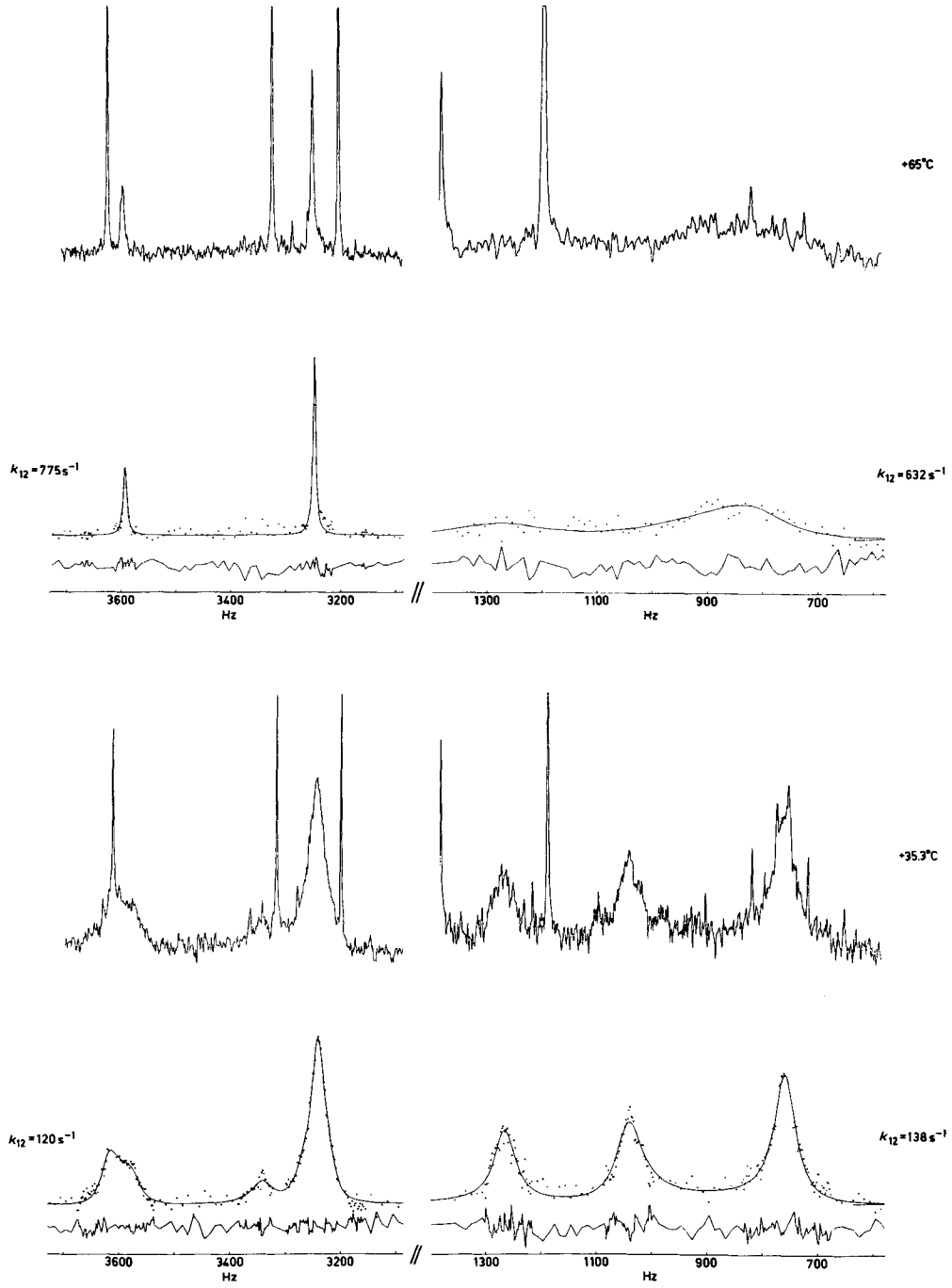

Fig. 9a. *Experimental and simulated spectra at 65.7 and 35.3°C* (Example D). To the left: vinyl; to the right: non-vinyl C-atoms. Extra lines not simulated refer to the decomposition product.

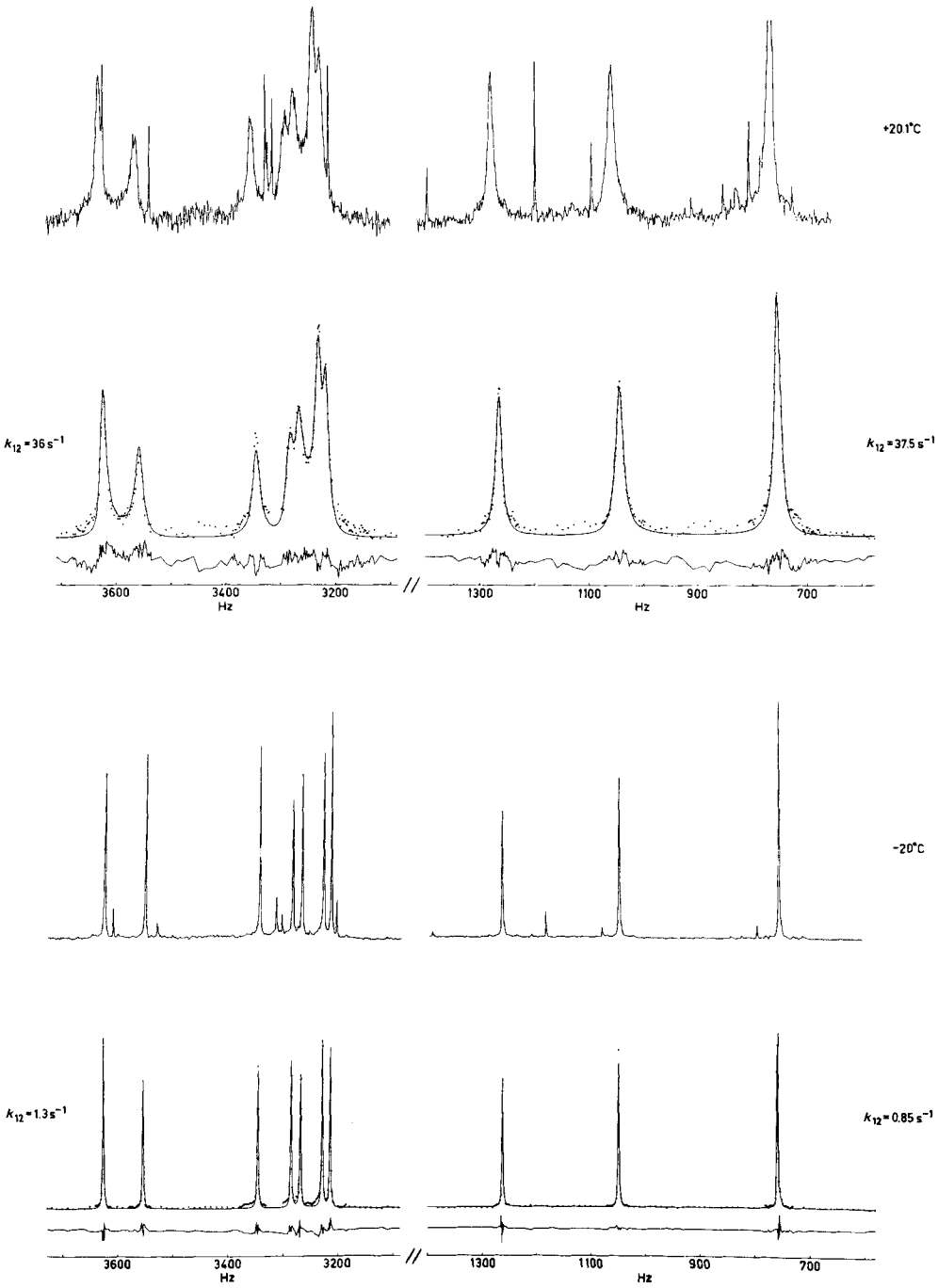

Fig. 9b. *Experimental and simulated spectra at 20.1 and −20°C* (Example D). To the left: vinyl; to the right: non-vinyl C-atoms. Extra lines not simulated refer to the decomposition product.

A representing choice of experimental and calculated spectra is shown in *Figures 9a* and *9b*.

The sensitivity plots $\log_{10}\Delta s_r$ *versus* $\log_{10}k_{12}$ for $r = G_{1,1}$, $\nu_{j,k}$, $\Delta\nu_2$, $\Delta\nu_5$, P_1, and k_{12} *(Fig. 10)* confirm the features already discussed in the preceding examples. The origin of the extra peaks near $k_{12} = 100\ s^{-1}$ is not known, they seem to be due to experimental inconveniencies.

The kinetic data for the reaction $II_1 \rightarrow II_2$ were obtained by weighted least-squares fitting of the rate constants k_{12} to the *Arrhenius* and *Eyring* equation, respectively. The kinetic data are collected in the first row of *Table 5*. Likewise, fitting $k_{21} = k_{12}P_1/(1-P_1)$ for the reaction $II_1 \leftarrow II_2$ to the corresponding equations yielded the kinetic data shown in the second row of *Table 5*. The last row contains the kinetic data of the equilibrium constant $K_{eq} = (1-P_1)/P_1 = \exp(-\Delta G°/RT)$.

Table 4. *Temperature dependence of the chemical shifts* (Example D)

Chemical shifts j,k	Tautomeric system $II_1 \rightleftharpoons II_2$		
	$\nu^0_{j,k}$ [Hz]	$b_{j,k}$ [Hz/°C]	Correlation
$\nu_{1,1}$	1263.4	0.117	0.9718
$\nu_{1,2}$	3344.4	−0.022	−0.4616
$\nu_{2,1}$	3623.7	−0.068	−0.8724
$\nu_{2,2}$	3553.0	0.056	0.7036
$\nu_{3,1}$	3228.1	0.001	0.0181
$\nu_{3,2}$	3268.0	0.022	0.3779
$\nu_{4,1}$	3214.4	0.047	0.5851
$\nu_{4,2}$	3284.5	−0.016	−0.3751
$\nu_{5,1}$	754.6	−0.017	−0.5844
$\nu_{5,2}$	1046.2	−0.050	−0.8918

Table 5. *Kinetic data of the tautomeric system* $II_1 \rightleftharpoons II_2$ (Example D).

Kinetic data of	E_A [kJ/mol]	$\log_{10}A$	$\Delta H^{\neq}$ [kJ/mol]	$\Delta S^{\neq}$ [J/(mol. Grad)]	$\Delta G^{\neq}$ (25°C) [kJ/mol]	K(25°C) [s^{-1}]
k_{12}	58.3 ±2.2[a])	11.9 ±0.38[a])	55.9 ±2.2[a])	−24.5 ±5.0[a])	63.21 ±0.44[a])	51.8 ±9.2[b])
k_{21}	58.3 ±2.2[a])	12.0 ±0.38[a])	55.8 ±2.2[a])	−22.7 ±5.4[a])	62.60 ±0.45[a])	65.5 ±11.8[b])
			$\Delta H°$	$\Delta S°$	$\Delta G°$ (25°C)	K (25°C)
K_{eq}[c])			−0.34 ±0.20[d])	−3.1 ±1.2[d])	0.60 ±0.15[e])	0.788 ±0.048[f])

[a]) The errors were calculated from $T_1 = 339$ K, $\sigma_{T_1} = \pm 0.5$ K; $T_2 = 253$ K, $\sigma_{T_2} = \pm 0.2$ K; $\sigma_{K_1}/K_1 = \pm 0.15$; $\sigma_{K_2}/K_2 = \pm 0.2$.

[b]) $\sigma_K/K = \sigma_{\Delta G^{\neq}}/RT$.

[c]) The errors of $\Delta H°$, $\Delta S°$, and $\Delta G°$ were calculated in an analogous way as those shown in the Appendix.

[d]) $(P_1)_1 = 0.58$, $(\sigma_{P_1})_1 = \pm 0.015$; $(P_1)_2 = 0.54$, $(\sigma_{P_1})_2 = \pm 0.015$.

[e]) $P_1 = 0.56$, $\sigma_{P_1} = \pm 0.015$.

[f]) $\sigma_K/K = \sigma_{\Delta G°}/RT$.

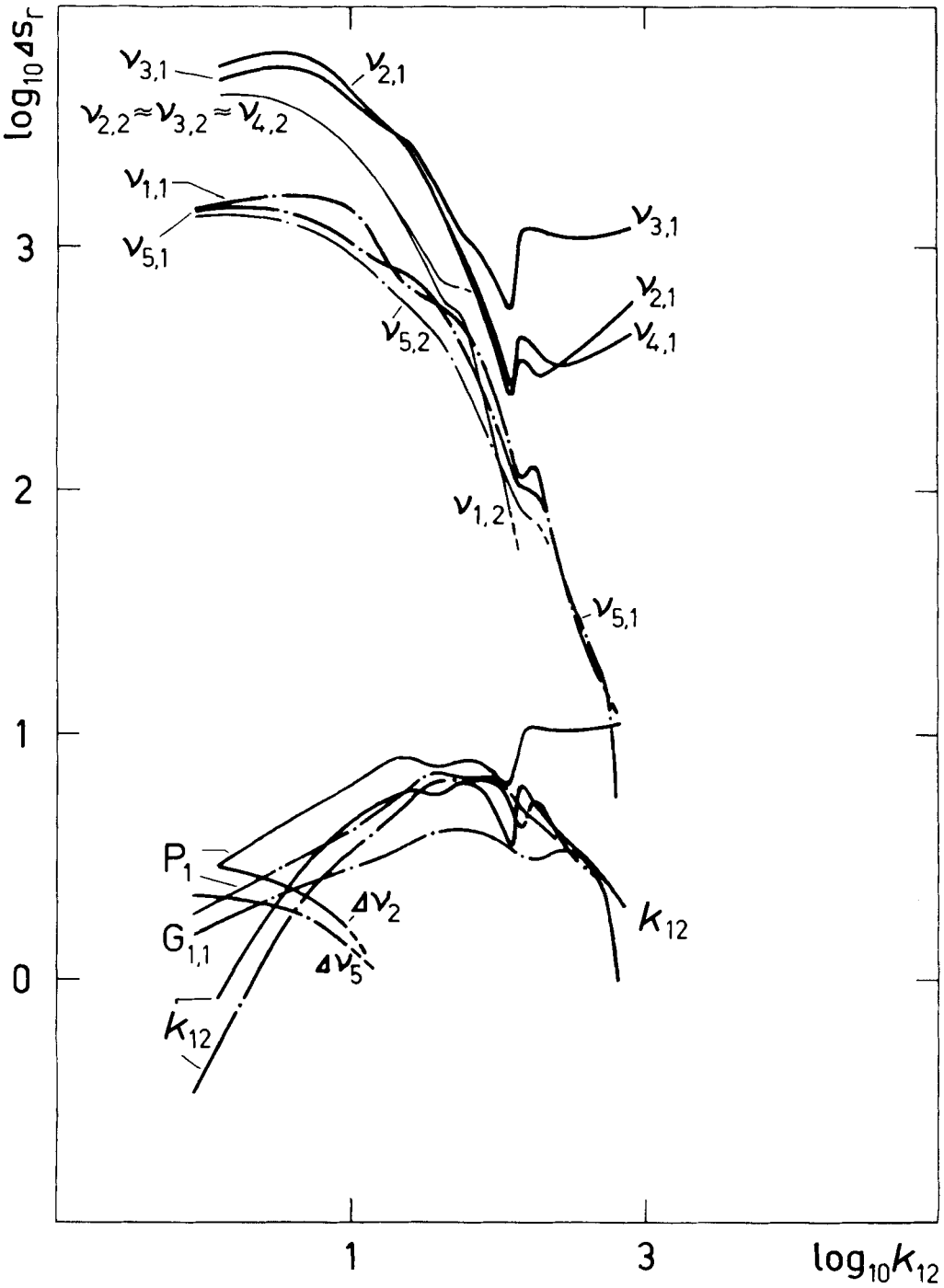

Fig. 10. *Parameter sensitivities of example D.* Dotted lines characterize parameters of the non-vinyl spectra. Thin lines refer to structure II_2.

Conclusions. – The four examples analysed by the program CNMREX demonstrate that rate constants covering a range of about 1 to 100,000 s^{-1} (related to maximum chemical shift separations of 260, 260, 270, and 2080 Hz, respectively) can be extracted from exchange-broadened lineshapes. The range of adjustable rate constants depends upon the maximum value of the chemical shift separations.

Least-squares fitting of ^{13}C-DNMR. spectra demands adjustment of all physically meaningfull parameters. Even a slight deviation of a chemical shift, for instance, may introduce large errors leading to incorrect rates. The supplementary expence is rewarded by additional data such as temperature dependence of the chemical shifts or site populations, apparent linewidths at slow or fast exchange as well as (accurate) populations. Finally, statistical data comprising parameter confidence limits, R factors, sensitivity measures, and a correlation matrix are calculated. The least-squares iterations converge easily provided that the parameters do not strongly correlate with each other. Strong correlation can be avoided by proper use of a parameter control vector. Optimizing as many significant parameters as possible usually proved to be most convenient and time saving.

There is no doubt that any digital spectra preprocessing such as base-line flattening, noise reduction, and smoothing (as has been outlined, for instance, by *Stephenson & Binsch* (18) would have led to a better agreement of the theoretical and experimental spectra of examples C and D. Future activities in spectra fitting certainely will take advantage of such techniques.

We believe that the iterative least-squares lineshape fitting described in this paper will contribute to a more straightforward computer supported evaluation of molecular dynamic data.

We wish to thank Dr. *H. Baumann* for helpful suggestions, Prof. *G. Binsch* for his critical review, and the computer center of the *Eidg. Techn. Hochschule Zürich* for the computing time.

Appendix. – *Error analysis of the kinetic data.* The error propagation formula [33]:

$$\sigma_x^2 = (\partial x/\partial u)^2 \sigma_u^2 + (\partial x/\partial v)^2 \sigma_v^2 + \ldots \tag{A1}$$

was taken in order to calculate the uncertainties in the kinetic data. Eq. (A1) assumes that the fluctuations in the observations of u and v, ... are uncorrelated [33]. The variances σ_z^2 are defined by:

$$\sigma_z^2 = \lim_{N \to \infty} (1/N) \sum_{i=1}^{N} (z_i - \bar{z})^2. \tag{A2}$$

Applying Eq. (A1) to the kinetic parameters A, E_A, $\Delta H^{\neq}$, $\Delta S^{\neq}$, and $\Delta G^{\neq}$ yields:

$$(\sigma_{\ln A}/\ln A)^2 = [T_1 T_2 D/(\Delta T E)]^2 [(\sigma_{T_1}/T_1)^2 + (\sigma_{T_2}/T_2)^2] + (T_1/E)^2 (\sigma_{K_1}/K_1)^2 + (T_2/E)^2 (\sigma_{K_2}/K_2)^2, \tag{A3}$$

$$(\sigma_{E_A}/E_A)^2 = (T_2/\Delta T)^2 (\sigma_{T_1}/T_1)^2 + (T_1/\Delta T)^2 (\sigma_{T_2}/T_2)^2 + (1/D)^2 [(\sigma_{K_1}/K_1)^2 + (\sigma_{K_2}/K_2)^2], \tag{A4}$$

$$\begin{aligned}(\sigma_{\Delta H^{\neq}}/\Delta H^{\neq})^2 = {} & (T_2/\Delta T + 1/\ln B)^2 (\sigma_{T_1}/T_1)^2 + (T_1/\Delta T + 1/\ln B)^2 (\sigma_{T_2}/T_2)^2 \\ & + (1/\ln B)^2 [(\sigma_{K_1}/K_1)^2 + (\sigma_{K_2}/K_2)^2],\end{aligned} \tag{A5}$$

$$\begin{aligned}(\sigma_{\Delta S^{\neq}}/\Delta S^{\neq})^2 = {} & [T_1/F + T_1 T_2 \ln B/(\Delta T F)]^2 (\sigma_{T_1}/T_1)^2 + [T_2/F + T_1 T_2 \ln B/(\Delta T F)]^2 (\sigma_{T_2}/T_2)^2 \\ & + (T_1/F)^2 (\sigma_{K_1}/K_1)^2 + (T_2/F)^2 (\sigma_{K_2}/K_2)^2,\end{aligned} \tag{A6}$$

$$(\sigma_{\Delta G^{\neq}}/\Delta G^{\neq})^2 = [1 + 1/\ln(C/K)]^2 (\sigma_T/T)^2 + [1/\ln(C/K)]^2 (\sigma_K/K)^2 \tag{A7}$$

with

$T = 298$ K;
$K = k(T)$;
$\Delta T = T_1 - T_2$;
$B = K_1 T_2/(K_2 T_1)$;
$C = \varkappa k_B T/h$, $\varkappa = 1$,
$k_B = 1.3804\ 10^{-16}$ erg Grad^{-1},
$h = 6.625\ 10^{-27}$ erg s;

$D = \ln K_1 - \ln K_2$;
$E = T_1 \ln K_1 - T_2 \ln K_2$;
$F = T_1 \ln(K_1/C_1) - T_2 \ln(K_2/C_2)$,
$C_1 = C\,T_1/T$, $C_2 = C\,T_2/T$;
$\sigma_T/T = (1/2)(\sigma_{T_1}/T_1 + \sigma_{T_2}/T_2)$;
$\sigma_K/K = (1/2)(\sigma_{K_1}/K_1 + \sigma_{K_2}/K_2)$.

T_1 refers to the highest, T_2 to the lowest temperature [K] used for the *Arrhenius (Eyring)* plot, $K_1 = k(T_1)$ and $K_2 = k(T_2)$, respectively, are their corresponding rates. σ_{T_1} and σ_{T_2} must be deduced from temperature measurements. σ_{K_1} and σ_{K_2} are estimated from the lineshape fitting.

Eqs. A3 through A7 have been implemented in the linear least-squares program NMRACP.

REFERENCES

[1] *Yu. K. Grishin, N. M. Sergeyev, O. A. Subbotin & Yu. A. Ustynyuk,* Mol. Phys. *25*, 297 (1973).
[2] *J. F. M. Oth, K. Muellen, J.-M. Gilles & G. Schroeder,* Helv. *57*, 1415 (1974).
[3] *F. A. Cotton, D. L. Hunter & P. Lahuerta,* J. Am. Chem. Soc. *96*, 7926 (1974); *F. A. Cotton & D. L. Hunter,* ibid. *98*, 1413 (1976).
[4] *L. Vancea, R. K. Pomeroy & W. A. G. Graham,* J. Am. Chem. Soc. *98*, 1407 (1976).
[5] *S. F. Nelsen & G. R. Weisman,* J. Am. Chem. Soc. *98*, 3281 (1976).
[6] *O. A. Gansow, A. R. Burke & W. D. Vernon,* J. Am. Chem. Soc. *98*, 5817 (1976).
[7] *R. P. Kirchen & T. S. Sorensen,* J. Am. Chem. Soc. *99*, 6687 (1977); ibid. *100*, 1487 (1978).
[8] *F. A. L. Anet & I. Yavari,* J. Am. Chem. Soc. *99*, 6986 (1977); ibid. *99*, 7640 (1977).
[9] *J. F. M. Oth, K. Muellen, H.-V. Runzheimer, P. Mues & E. Vogel,* Angew. Chem. *89*, 910 (1977).
[10] *K. K. Curry & J. W. Gilje,* J. Am. Chem. Soc. *100*, 1442 (1978).
[11] *J. Jonáš, A. Allerhand & H. S. Gutowsky,* J. Chem. Phys. *42*, 3396 (1965).
[12] *B. G. Cox, F. G. Riddell & D. A. R. Williams,* J. Chem. Soc. (B), *1970*, 859.
[13] *J. Gelan,* J. Magn. Res. *10*, 37 (1973).
[14] *O. Yamamoto, M. Yanagisawa, K. Hayamizu & G. Kotowycz,* J. Magn. Res. *9*, 216 (1973).
[15] *D. L. Lichtenberger & T. L. Brown,* J. Am. Chem. Soc. *99*, 8187 (1977).
[16] *S. O. Chan and L. W. Reeves,* J. Am. Chem. Soc. *95*, 670 (1973); ibid. *95*, 673 (1973); and references therein.
[17] *D. S. Stephenson and G. Binsch,* J. Magn. Reson. *32*, 145 (1978).
[18] *D. S. Stephenson and G. Binsch,* J. Magn. Reson. *37*, 395, 409 (1980).
[19] *G. Binsch and H. Kessler,* Angew. Chem. *92*, 445 (1980).
[20] *D. W. Marquardt,* J. Soc. Ind. Appl. Math. *11*, 431 (1963).
[21] *J. Heinzer,* J. Magn. Reson. *26*, 301 (1977).
[22] *A. Jones,* Comput. J. *13*, 301 (1970).
[23] *R. A. Sack,* Mol. Phys. *1*, 163 (1958).
[24] *J. Heinzer,* Mol. Phys. *22*, 167 (1971).
[25] *J.-M. Gilles,* Thèse de doctorat (physique), Université Libre de Bruxelles 1969.
[26] *R. G. Gordon & R. P. McGinnis,* J. Chem. Phys. *49*, 2455 (1968).
[27] *G. Binsch,* J. Am. Chem. Soc. *91*, 1304 (1969).
[28] *J.-M. Gilles and J. F. M. Oth,* Program LSHKUBO.
[29] *J. Heinzer,* J. Magn. Reson. *13*, 124 (1974).
[30] *V. S. Dimitrov,* J. Magn. Reson. *22*, 71 (1976).
[31] *R. Laatikainen,* J. Magn. Reson. *27*, 169 (1977).
[32] *Y. de Julien de Zélicourt,* Thesis ETHZ, Nr. 5679 (1976).
[33] *P. R. Bevington,* Data Reduction and Error Analysis for the Physical Sciences, McGraw-Hill Book Company, New York, 1969.
[34] *S. W. Staley & T. J. Henry,* J. Am. Chem. Soc. *92*, 7612 (1970).
[35] *K. Muellen,* privat communication.